Journal of Engineering Mechanics and Machinery (2026)
Clausius Scientific Press, Canada

DOI: 10.23977/jemm.2026.110107
ISSN 2371-9133 Vol. 11 Num. 1

Research on Static Strength Design of Automotive Drive Shafts Based on Strength Fields

Tong Li[1,*]

[1]*School of Mechanical Engineering, University of Shanghai for Science and Technology, Shanghai, China*
[*]*Corresponding Author: 2549643603@qq.com*

Keywords: Drive Shaft, Strength Fields, Full-Field Stress-Strain Interference Model, Quenching Characteristics

Abstract: Taking a certain automotive transmission intermediate shaft as an example, the mismatch between the structural stress field and overall strength in strength design theory, coupled with the lack of relevant theoretical and technical basis for quantitative alignment between design and manufacturing, leads to localized strength excess in structural design and manufacturing. This paper proposes a comprehensive strength design theory and methodology based on structural strength fields and full-field stress-strength interference theory. by solving for maximum stress and its gradient direction stress distribution alongside the strength distribution curve in that direction, and utilizing the full-field stress-strength interference model and the end-hardening characteristics of structural materials, the optimal location of critical points is designed while minimizing local strength excess in subsurface and core regions. The final design results demonstrate: The critical point is located 2.6 mm from the surface, reducing strength excess by 529 MPa at this point; At the core position 4.5 mm from the surface, strength excess is reduced by 686 MPa, effectively resolving localized strength excess issues. Static strength tests were conducted on the strength-matched drive shaft. Test results confirm that the shaft meets all static strength requirements post-matching, validating the correctness and feasibility of this methodology.

1. Introduction

With the rapid development of China's manufacturing sector, construction machinery has emerged as a key industry in implementing the Industrial Product Quality Enhancement Action Plan under Made in China 2025. Concurrently, standards for industrial product performance and quality continue to rise, while requirements for rational and scientific product design are becoming increasingly standardized. Among the numerous performance requirements in mechanical design, static strength represents a fundamental property that mechanical structural components must satisfy during design. Whether subjected to static or dynamic loads, mechanical structures must first meet static strength design requirements.

Through continuous in-depth research by scholars both domestically and internationally, current studies on structural static strength design methods primarily focus on two directions: establishing

design models via theoretical approaches for static strength optimization design, and investigating the influence of materials and manufacturing processes on strength, subsequently applying these insights to structural static strength design. R Das et al. [1] employed the ESO algorithm for structural static strength optimization design, utilizing an approximate method to evaluate fracture-related stress intensity factors for static strength design of shoulder radii under uniaxial tension; Matteo Gavazzoni et al. [2] developed a GTN model for designing the static strength of metallic lattice structures, investigating numerical prediction of multi-axial static strength for lattice structures; Liao Shanbin [3] et al. explored a flywheel static strength analysis method based on static safety factors, utilizing the principle that relative stress gradients modify material allowable stresses, effectively avoiding structural over-strengthening and reducing flywheel weight; Chang Nan et al. [4] coupled variable-accuracy modeling of aircraft structures with static strength design, proposing a structural design method that balances multiple constraints including static strength and durability.

In the application of materials and manufacturing to structural static strength design, P N Parkes et al. [5] investigated the static strength of metal composite nodes with penetrating reinforcement; G Xiao et al. [6] proposed a novel method using auxiliary sheet reinforcement (ASR) to enhance joint strength, employing auxiliary thin plates made of four materials. experimentally investigating their effects on joint strength. X Lan et al. [7] employed an established finite element model to study the static strength of high-strength steel (CHS) X-type joints under axial compression loads, as well as the material properties of CHS X-type joints under various nominal stresses.

However, analysis of domestic and international research on structural static strength design reveals that existing approaches are based on engineering mechanics—specifically, the safety factor/allowable stress framework. This framework focuses on overall strength design and material-manufacturing matching centered on the point of maximum stress (design point/critical point). Strength is treated as an experimental average and holistic value. Under the assumption of overall strength, the critical point is directly identified as the point of maximum stress. This approach prevents active design targeting critical points on hazardous sections and fails to quantitatively allocate strength design parameters to material-manufacturing parameters. Furthermore, safety considerations often lead to the adoption of large safety factors in design, exacerbating issues such as excessive lightweighting potential and over-provision of local structural strength. Therefore, conducting design-matching research based on strength gradients/fields is crucial for addressing the local strength redundancy in critical sections caused by traditional strength design approaches focused on overall strength.

This paper proposes a structural static strength design theory and methodology based on full-field strength. Addressing the limitations in structural strength design under overall strength conditions, it treats strength according to its non-uniform characteristics. This study introduces the concept of an intensity field and constructs a model to characterize static intensity fields. It extends the full-field stress-strength interference model by treating the static strength of mechanical structures and components as fields, thereby organically matching the structural stress field with the static strength field. This approach effectively reduces local strength excess and increases material strength utilization. Using the intermediate shaft of an isokinetic universal joint transmission as an example, the paper demonstrates full-field static strength design for structures. The validity and feasibility of the proposed method are verified through static strength testing.

2. Design theory

2.1 Strength field theory and characterization models

Analysis of factors influencing strength reveals that a material's chemical composition, microstructure, grain size, and various heat treatment manufacturing processes significantly impact

its strength magnitude. Structural strength is not uniformly distributed throughout the material. Following material-manufacturing processes, strength distribution exhibits a gradual decrease from the surface toward the core, presenting an uneven gradient distribution. Particularly in components subjected to carburizing, a carbon concentration gradient forms from the surface to the subsurface. This results in a sharp increase in surface strength relative to the core, manifesting as an uneven strength distribution. The essence of mechanical manufacturing lies in the evolution of strength gradients through the overall or localized strengthening or weakening of the blank. Strength exhibits a field property, meaning the strength at every point within the structure is distinct.

By establishing a strength field characterization model, the true strength value at every point within the structure can be accurately reflected. However, the strength field varies across different materials and manufacturing processes, necessitating a comprehensive consideration of both the material's inherent strength and the strengthening or weakening effects of manufacturing. A preliminary static strength field model is established as follows:

$$\sigma_{b(i,j,k)} = \sigma_{b0(i,j,k)} \prod_{m=1}^{n} k_m \tag{1}$$

In the formula, $\sigma_{b(i,j,k)}$ denotes the static strength at any point (i,j,k) in the structure; $\sigma_{b0(i,j,k)}$ denotes the material-determined static strength at any point (i,j,k); K_m represents the comprehensive influence coefficient of the mth manufacturing process on static strength; n denotes the number of manufacturing processes.

Although the static strength of a structure determined by its material can be obtained through strength testing, the strength results derived from testing represent the overall effect of structural failure. They do not yield the strength at any specific point within the structure; essentially, they provide the overall strength. This overall strength cannot reflect the actual conditions nor express the true strength value at every point within the structure. However, by conducting hardness testing, the hardness field distribution of the structure can be measured. Combining this with the hardness-strength conversion relationship ultimately yields a static strength field model characterized by the hardness field:

$$\sigma_{b(i,j,k)} = C_{(i,j,k)} \times H_{(i,j,k)} \tag{2}$$

In the formula, $H_{(i,j,k)}$ represents the hardness at any point (i,j,k) of the part; $C_{(i,j,k)}$ denotes the conversion relationship between hardness and static strength at any point (i,j,k) of the mechanical part.

Taking a typical quenched structure as an example, the hardness field can be determined using the end-hardening curve method to derive a static strength characterization model. Representative end-hardening curve formulas include the USS-Atlas formula, the Yu-Baihai formula, and the Jin-Man formula. This paper employs the Jin-Man formula as a bridge to characterize the static strength model. The hardness field calculation formula is as follows [8]:

$$J(x) = \begin{cases} J_{\max} & 0 \le x < b \\ \dfrac{\left(J_{\max} - J_{\min}\right)}{\left(x-b\right)^2 / \left[3\left(h-b\right)^2\right] + 1} + J_{\min} & x \ge b \end{cases} \tag{3}$$

In the equation, $J(x)$ represents the end-hardened hardness; x denotes the end-hardening distance; J_{max} indicates the maximum hardness on the end-hardening curve; J_{min} signifies the minimum hardness on the end-hardening curve; b is the length of the martensite zone obtained at the specimen end; h is the hardenability coefficient, whose geometric meaning is the distance from the origin to the

inflection point of the curve.

In summary, the hardness field prediction model derived from the Jinman empirical formula, combined with the hardness-strength conversion relationship, yields the following static strength field model characterized by hardness:

$$\sigma_b(x) = C \times J(x) \tag{4}$$

2.2 Full-field stress-strain interference theory

In mechanical strength and reliability design, whether a component functions normally or fails depends on the relationship between strength and stress. When a component's strength is greater than or equal to the stress, it can operate normally; when its strength is less than the stress, failure occurs. Therefore, stress-strength interference essentially involves comparing the relationship between stress and strength—that is, the full-field interference between the stress field and the strength field. This encompasses interference comparisons at all points within three-dimensional space. By establishing a one-to-one stress-strength comparison relationship at each spatial location, the stress at any point is compared with its corresponding strength. This enables the determination of structural safety or the prediction of failure risk.

When the stress field distribution is deterministic, and the strength field follows a deterministic distribution, the maximum stress and its gradient direction on the critical structural section can be determined through mechanical equations or simulation. The strength distribution along the same gradient direction can be obtained via end-quench testing combined with hardness measurement. By mapping both stress and strength distributions onto a common coordinate system, their variations with position (depth) along the gradient direction become visible. Each position corresponds to a stress value and a strength value. By comparing the stress at any point with the strength at that point, the location of critical points can be identified and actively designed. This constitutes the primary function of stress-strength interference: location-dependent distribution and interference—active design and identification of critical points.

A critical point refers to the location within a structure most susceptible to failure or damage, representing the weakest design point among all structural locations. By comparing all points along the gradient direction of the critical section, it is determined that the critical point of the structure lies at the position where the stress distribution and strength distribution along the gradient direction are closest. Let point $Q(i_0,j_0,k_0)$ be the critical point of the structure. Then the strength $f_{strength}(i_0,j_0,k_0)$ and stress $f_{stress}(i_0,j_0,k_0)$ at this point must satisfy:

$$\left| \frac{f_{strength}(i_0, j_0, k_0)}{f_{stress}(i_0, j_0, k_0)} \right| = \min \left| \frac{f_{strength}(i, j, k)}{f_{stress}(i, j, k)} \right| \tag{5}$$

Therefore, it is only necessary to determine the maximum stress and its gradient direction stress distribution at the structurally critical section, along with the corresponding strength distribution in that gradient direction. Based on the stress-strength interference model combined with Equation (5), the location of the critical point can be identified.

It is worth noting that whenever the stress distribution or strength distribution changes, the location of critical points will also shift. In the strength design process of mechanical structures, the stress gradient distribution—typically determined by the load and structural configuration—remains fixed. Strength design requirements are generally met through material selection and manufacturing process treatments, meaning critical points are proactively designed by altering the strength distribution curve.

Assuming the maximum stress distribution curve along the gradient direction of the hazardous

section is denoted as *f(x)*, and the minimum strength distribution curve along the same gradient direction is denoted as *g(x)*, the strength margin $S_{(x_0)}$ at any point x0 on the gradient distribution curve is mathematically expressed as:

$$S_{(x_0)} = \left| f(x_0) - g(x_0) \right| \tag{6}$$

In practical engineering applications, when the stress field distribution follows a random distribution and the strength field distribution is a combination of random distributions, the strength and stress of a component are random variables subject to specific distributions. The stress at any point in the structure varies with random load changes during use, while the strength at that point fluctuates due to random variations in material properties and manufacturing processes. When applying the primary aspect of stress-strength interaction—proactive design and assessment of critical points—to determine their locations, subsequent reliability design for these points involves stresses and strengths at critical points that also follow specific statistical distributions. This manifests as the secondary aspect of stress-strength interaction: probability distribution and interference. To be precise, it involves probability distributions and interference that vary with load, material, and manufacturing—reliability and safety design.

3. Materials and methods

This paper takes a certain automotive drive shaft as an example, featuring a hollow structure with variable cross-section and wall thickness, with a minimum diameter of 25.6 mm. The product's structural dimensions are shown in Figure 1. The drive shaft assembly requirements are as follows: when the fixed end has a swing angle of 40 ° and the sliding end has a swing angle of 10 °, under a loading speed of 180°/min, the failure torque must be ≥3700 N·m.

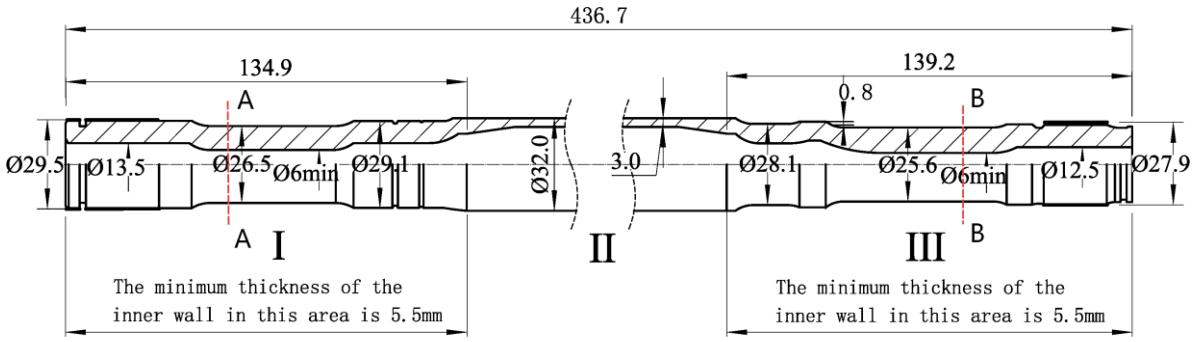

Figure 1 Drive shaft structural dimensions

The material grade is 25CrMo4, with its chemical composition shown in Table 1. The end-hardening curve distribution is illustrated in Figure 2.

Table 1 Chemical composition of 25CrMo4 (%, Mass fraction)

C	Mn	Si	Cr	Mo	Cu	P	S
0.22~0.29	0.60~0.90	≤0.40	0.90~1.20	0.15~0.30	≤0.25	≤0.035	≤0.035

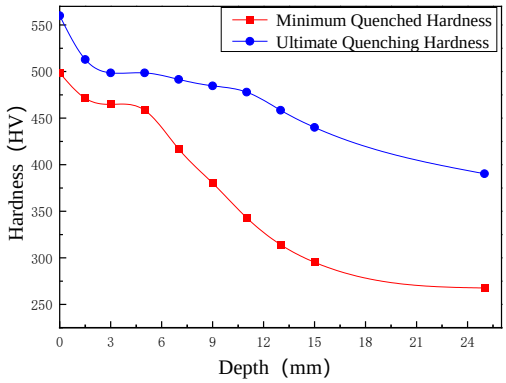

Figure 2 Distribution of quenching curves for 25CrMo4

Based on the characteristics of strength non-uniformity and incorporating full-field stress–strength interaction, this paper proposes a design method for the full-field static strength distribution of a structure. The steps are as follows:

First, the maximum static stress and its gradient direction at the critical section are calculated based on load characteristics and geometric features; second, based on the distribution of the maximum static stress and its gradient, the ideal static strength field distribution for the critical section is designed; Subsequently, using the ideal static strength field as a target, the actual static strength field distribution is matched by considering the material's end-hardening characteristics and manufacturing processes, and the design of critical points and determination of heat treatment process parameters are carried out; finally, based on full-field stress-strength interference analysis, an integrated evaluation and verification of strength design and material-manufacturing parameters are performed.

4. Results and analysis

4.1 Maximum static stress at the critical section and its gradient direction stress distribution

Due to the angular offset between the transmission intermediate shaft and the universal joint, a secondary bending moment is generated internally within the intermediate shaft during torque transmission to balance the torque transfer. The magnitude of this secondary bending moment can be derived from Equation (7) [9]:

$$M_w = M_n \mathrm{tg}\frac{\delta}{2} \tag{7}$$

In the formula, M_w represents the secondary bending moment; M_n denotes the transmitted torque; δ is the angle between the universal joint and the intermediate shaft.

The stresses in a hollow shaft under bending and torsion can be determined by applying knowledge of materials mechanics in conjunction with the third theory of strength. This allows for the calculation of stresses at every point along the gradient (depth) direction within the cross-section, as shown in Equation (8):

$$\tau_\rho = \frac{64M_n\rho\sqrt{1+\left(\tan\delta\right)^2}}{\pi D^4\left(1-\alpha^4\right)} \tag{8}$$

In the equation, τ_ρ is the stress at any point on the cross-section; ρ is the distance from a point to the center of the circular shaft; D is the diameter of the outer surface of the circular shaft; α is the ratio

of the inner diameter to the outer diameter.

Based on the assembly conditions, the ultimate torsional load borne by the drive shaft is 3700 N·m. With a fixed end swing angle of 40° and a sliding end swing angle of 10°, the critical section is determined to be section B-B—the smallest diameter section—with a diameter of 25.6 mm, as indicated by the cross-sectional dimensions of the intermediate shaft. Using Equation (8), the stress at any point on the critical section B-B is obtained as:

$$\tau_\rho = \frac{64.9 M_n \rho}{\pi D^3 (1-\alpha^4)} \approx 189.1\rho \tag{9}$$

From Equation (9), the maximum static stress and its gradient direction in the critical section of a hollow drive shaft under ultimate bending-torsion combined loading are obtained, with the maximum stress reaching 2420.5 MPa.

4.2 Design of ideal static strength field distribution for hazardous sections

The ideal static strength distribution represents the optimal solution for static strength design. It determines the ideal static strength field distribution of a structure based on the maximum static stress under ultimate static load during structural service and the stress distribution along its gradient direction. When the static strength at every point on the critical section's static strength distribution equals the ultimate stress at that point—that is, when the ultimate static stress distribution coincides with the static strength distribution on the critical section—this static strength distribution is termed the ideal static strength field distribution. At every point on the ideal static strength distribution of the critical section, the static strength satisfies the strength requirement without excess strength, achieving maximum strength utilization.

At the same time, considering that structural stress fluctuations may occur during service due to load variations, potential errors in mechanical analysis, discrepancies in material strength specifications, and other unforeseeable factors, a safety margin must be incorporated into the design. To this end, the maximum stress and its gradient distribution are multiplied by a safety factor n greater than 1, ensuring the structure operates safely.

Therefore, the ideal static strength distribution at the critical cross-section of the structure is determined by multiplying the maximum static stress and its gradient distribution by the safety factor. For this example, a safety factor of 1.2 is applied. The ideal static strength distribution at the critical cross-section of the drive shaft under ultimate bending-torsion loading is shown in Figure 3.

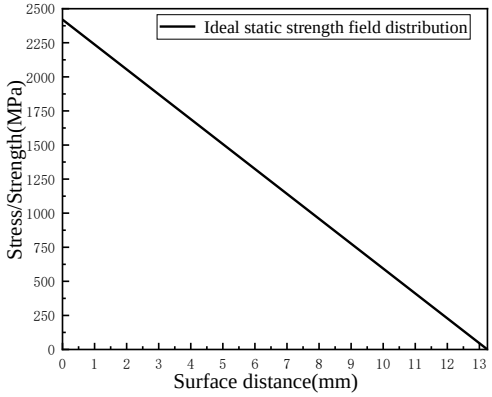

Figure 3 Ideal static strength distribution at critical section

4.3 Actual static strength field distribution matching

The ideal static strength field distribution at structurally critical sections exhibits no excess strength, maximizing the utilization of the material's static strength. However, due to limitations in materials and manufacturing processes, it is impossible to achieve this ideal static strength field through material and process matching. With the ideal static strength field as the target, the actual static strength field distribution is designed by matching material parameters and manufacturing process parameters. This ensures that the actual static strength field distribution determined by materials and manufacturing processes aligns as closely as possible with the ideal static strength field distribution. Consequently, the strength surplus in the actual static strength field is minimized, thereby enhancing the utilization rate of the material's static strength.

The design of the actual static strength field distribution essentially applies the principle of stress-strength interference primacy, equivalent to actively designing critical points by adjusting material and manufacturing parameters. For this example, with known material conditions and a defined manufacturing process, the actual static strength field distribution design determines the minimum and maximum hardness distribution curves based on the material's end-hardening characteristics. It then establishes the surface hardness and core hardness values. By integrating the hardness-strength conversion relationship, the minimum and maximum strength distribution curves are derived.

Using the minimum strength distribution curve as the design basis, the designed strength gradient curve is divided into three segments: A, B, and C. Segment A's length corresponds to the hardened layer depth, with its magnitude representing surface strength. Segment B serves as the transition zone derived by translating the strength of the end-quench curve. Section C represents the non-hardened zone, whose magnitude corresponds to the core strength. Under constraints of surface and core strength, the strength gradient design is primarily achieved by increasing or decreasing the hardened layer depth. This operation is equivalent to shifting the transition and non-hardened zones collectively to the right or left, thereby enabling proactive design of critical point locations. While avoiding excessive static strength in the surface, subsurface, and core regions, the final process parameters—including surface strength, core strength, hardened layer depth, and critical point Q location—are determined. This ensures the designed static strength distribution intersects the ideal static strength distribution at the surface or tangentially within the core, achieving optimal alignment.

Based on the aforementioned matching method, the 25CrMo4 material undergoes a heat treatment process of carburizing and quenching followed by low-temperature tempering. The corresponding heat treatment process parameters are specified in Table 2.

Table 2 Heat treatment requirements for intermediate shaft material 25CrMo4

Materials	Surface hardness (HV)	Hardened layer depth (mm)	Core hardness (HV)	Hazard point depth from surface (mm)
25CrMo4	538	1.1	467	2.6

According to the heat treatment requirements for 25CrMo4 material in Table 2, at the critical section B-B, after simultaneous carburizing and quenching of both inner and outer walls, the actual static strength gradient distribution is obtained as shown in Figure 4. This is derived from the material's quenching curve combined with the hardness-strength conversion relationship. In this case, based on experimental data, the conversion relationship between hardness and strength for the drive shaft is 1HV = 4.63MPa.

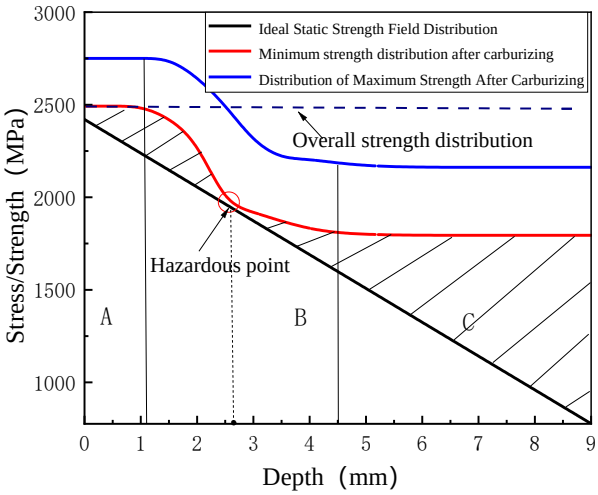

Figure 4 Actual static strength distribution

4.4 Strength evaluation and verification

Based on the material end-quench curve combined with the corresponding hardness-strength conversion relationship, the actual strength distribution for 25CrMo4 material was obtained. The designed ideal strength distribution was then established in the same coordinate system, as shown in Figure 5. Applying full-field stress-strength interference theory, quantitative evaluation and verification were conducted for the surface, subsurface, critical points, and core strength of the structure.

Specifically, the ideal surface strength of the drive shaft is 2420.5 MPa, while the corresponding actual surface strength is 2492 MPa. This indicates that after heat treatment matching, the surface strength of the structure meets requirements, and its performance is fully realized.

The ideal strength at the 1.5mm subsurface layer is 2146.4 MPa, with an actual strength of 2430 MPa, meeting strength requirements. This represents a slight reduction of 62 MPa compared to the overall design strength of 2492 MPa.

At the critical point 2.6mm from the shaft surface, the ideal strength is 1944 MPa; the actual strength is 1963 MPa, meeting strength design requirements and fully utilizing performance. Compared to the overall strength design of 2492 MPa, the critical point exhibits an excess strength reduction of 529 MPa.

At 4.5mm into the shaft core, the ideal strength is 1598.4 MPa. The actual core strength is 1806 MPa, meeting the strength design requirements and fully utilizing performance. Compared to the overall strength design of 2492 MPa, the core strength surplus is reduced by 686 MPa.

Analysis of the above design results indicates that the strength of the 25CrMo4 transmission shaft, after matching manufacturing process parameters, fully meets the strength design requirements.

4.5 Experimental verification

To further validate the correctness and feasibility of the theoretical methodology, the constant velocity universal joint shaft, which underwent full-field structural static strength design, was subjected to static strength testing in accordance with the requirements specified in GKN ADD 401010. The test conditions included a fixed-end swing angle of 40 °, a sliding-end swing angle of 10 °, and a loading speed of 180 °/min. The Nubia 1.8L/MT (L-Car) was tested under these parameters. Test numbers 09#, 10#, 11#, 12# were conducted using a 10k N·m static torsion strength test rig (567-014), as shown in Figure 5. Photographs of the fractured driveshaft after testing are presented in

Figure 6.

Figure 5 Static strength test equipment

Figure 6: Damage pattern of drive shaft assembly after static torsional strength test

The static strength test results for the drive shaft are shown in Table 3.

Table 3 Static strength test results

Number	**Permanent deformation (°)**	**Breakaway torque (N·m)**	**Average breaking torque (N·m)**
09#	0.81	4330	4234
10#	0.65	4044	
11#	0.66	4287	
12#	0.71	4275	

The static strength test results for the constant velocity universal joint drive shaft assembly indicate that failure occurred at the minimum diameter cross-section of the intermediate shaft, consistent with the theoretically identified critical section. Test data for the same material exhibited minimal variation and low dispersion, confirming the accuracy of the test results. When the stress corresponding to the drive shaft torque exceeds the structural strength, structural failure occurs. As shown in Table 3, the failure torques from the four test runs were 4330 N·m, 4044 N·m, 4287 N·m, and 4275 N·m, respectively. All values met the test requirement of drive shaft failure torque ≥ 3500 N·m.

5. Conclusion

This paper takes automotive transmission intermediate shafts as a case study. Based on strength field theory and characterization models, combined with full-field stress-strength interference theory, it proposes a structural static strength design method for full-field strength. Following this method and transmission shaft static strength test requirements, the shaft strength design was conducted, yielding the following conclusions:

(1) After matching manufacturing process parameters, the actual structural strength of the transmission shaft made from 25CrMo4 material consistently exceeds the structural stress, satisfying static strength design requirements;

(2) The proposed full-field strength structural static strength design method enables proactive design at critical points and strength matching at non-critical points based on material-manufacturing characteristics. This resolves the issue of local strength excess caused by existing holistic strength-based design approaches. Compared to traditional strength design methods, critical point strength excess is reduced by 529 MPa, and core strength excess is reduced by 686 MPa. This effectively minimizes structural strength redundancy and enhances material strength utilization;

(3) The feasibility of the full-field strength structural static strength design method was validated through transmission intermediate shaft assembly testing, providing theoretical and technical guidance for static strength design of other critical automotive components in practical engineering applications.

Meanwhile, during the research process, it was found that due to the randomness of the hardness measurement points, measurement equipment, measurement methods, or technicians and other random factors, the data of the hardness-strength conversion results fluctuated. It is necessary to conduct multiple measurements as much as possible, and use the average value results to ensure the accuracy of the strength design. Furthermore, the full-field static strength design method was extended to the structural fatigue strength design, and the universality of the design theory was further demonstrated.

References

[1] DAS R, JONES R, XIE Y M. Design of structures for optimal static strength using ESO[J]. Engineering Failure Analysis, 2004, 12(1): 61-80.

[2] MATTEO G, MARCO P, STEFANO B. Multiaxial static strength of a 3D printed metallic lattice structure exhibiting brittle behavior[J]. Fatigue & Fracture of Engineering Materials & Structures, 2021, 44(12): 3499-3516.

[3] Liao Shanbin, Xu Yingtao, Zeng Xiaochun. Static Strength Analysis Method for Flywheels Based on Static Safety Factor [J]. Diesel Engine Design and Manufacturing, 2023, 29(04): 19-22.

[4] Chang Nan, Xu Rongxin, Chen Xianmin. Preliminary Structural Optimization Method for Strength/Durability [J]. Acta Aeronautica et Astronautica Sinica, 2021, 42(05): 347-357.

[5] PARKES P N, BUTLER R, MEYER J, et al. Static strength of metal-composite joints with penetrative reinforcement[J]. Composite Structures, 2014, 118: 250-256.

[6] XIAOLEI G, CHAO C. A novel strengthening process to improve the strength of AL5052 square clinched joint[J]. The International Journal of Advanced Manufacturing Technology, 2023, 125(7-8): 3527-3538.

[7] LAN X, CHAN T-M, YOUNG B. Static strength of high strength steel CHS X-joints under axial compression[J]. Journal of Constructional Steel Research, 2017, 138: 369-379.

[8] Jin Man, Lian Jianshe, Jiang Zhonghao. A New Method for Predicting End Quench Curves of Structural Steel [J]. Acta Metallurgica Sinica, 2006, (04): 405-410.

[9] Lu Xi, Zhang Zhendong. Vibration Analysis of Ball Cage Constant Velocity Joints [J]. Bearing, 2002(08): 28-30.